2.5 MECHANICAL PROPERTIES CHARACTERIZATION OF A LARGER BEST PRACTICE HEAT OF 14YWT NFA1 – M.E. Alam, N. J. Cunningham, D. Gragg, K. Fields, G. R. Odette (UCSB), D. T. Hoelzer (ORNL) and S. A. Maloy (LANL)

OBJECTIVES

The objective of this study is to characterize the microhardness, tensile properties and fracture toughness of a newly developed larger best practice heat of 14YWT nanostructured ferritic alloys.

SUMMARY

A new larger heat of best practice nanostructured ferritic alloy (NFA), designated FCRD NFA1, was produced by ball milling argon atomized Fe-14Cr-3W-0.4Ti-0.2Y (wt.%) and FeO powders followed by consolidation and thermomechanical processing sequence of extrusion (850°C), annealing and cross-rolling (1000°C) steps. The microhardness of NFA1 averaged ≈ 376 ± 18 (kg/mm^2). The corresponding uniaxial tensile yield stress and ductility from 22 to 800°C are high at >1000 MPa at 22°C to >500 MPa at 600°C and 15-25%, respectively. K_{Jc}(T) fracture toughness curves were also measured from -196 to 22°C using pre-cracked 3-point bend (3PB) specimens. NFA1 manifests an exceptionally low fracture toughness transition temperature of ≈ -175°C in both LT and TL orientations. These results represent an *extraordinary combination* of strength and toughness. Extensive fractography provided insight on key fracture mechanisms.

BACKGROUND

Advanced fission and future fusion energy depends on developing new, high performance structural materials that can sustain extended component lifetimes under extreme conditions. Nanostructured ferritic alloys (NFA) are well known for their unique features such as exceptional thermal stability, outstanding high temperature strength and remarkable irradiation tolerance, including managing high concentrations of helium. These outstanding attributes are provided by an ultrahigh density of nm-scale Y–Ti–O rich oxide nanofeatures (NFs) [1]. The conventional NFA processing path is ball milling to mechanically alloy Y_2O_3 in the Fe-Cr(-W-Ti) matrix, which is an expensive process and often leads to heterogeneous distributions of NFs [2]. To try to overcome these limitations, an alternative processing path in which Y is included in the melt prior to gas atomization and rapid solidification was developed in collaboration with partner institutions including Oak Ridge National and Los Alamos National Laboratories, under the sponsorship of the DOE Office of Nuclear energy. ATI Powder Metals provided atomized Fe-14Cr-3W-0.4Ti0.2Y powders. However, the Y was phase separated after atomization, this low interstitial alloy powder variant was ball milled for 40 hours with FeO to increase the O content, by Zoz GMBH (Germany). The milled powders were processed at ORNL by canning, degassing and extruding at 850°C, followed by annealing (0.5 h) and cross-rolling (50% thickness reduction) at 1000°C. The larger scaled up alloy of 14YWT, called FCRD NFA1, followed the same processing route as a previous smaller developmental heat called 14YWT-PM2 [3]. Microstructural characterization studies on PM2 and NFA1, including SANS, APT, TEM, have been previously reported [2]. Mechanical property characterizations that included microhardness, tensile and fracture toughness are reported here. Fracture surfaces were also characterized by SEM fractography.

EXPERIMENTAL

Microhardness testing was performed on the flat and polished surfaces using a Vickers indenter and 500g load on a LECO M-400A semi-automated hardness tester. Seven randomly selected specimens were chosen and 10 to 15 indents were made in each specimen. Tensile testing was performed on the dog-bone shaped SSJ2 (5.0x1.2x0.5 mm^3) specimens both at longitudinal (L) and transverse (T) directions (Figure 1) at temperatures ranging from 22 to 800°C using a 810 MTS servo-hydraulic universal testing machine with a crosshead speed of 0.12 mm/min (strain rate of 4 x 10^{-4}/s). Fracture tests were conducted

from -196 to 22°C on fatigue pre-cracked single-edged notch three point bend (3PB) bars (3.33x3.33x18 mm^3) (Figure 1). The tests were conducted in general accordance with the ASTM 1921 standard practice. The K_{Jc} were calculated at the maximum load, often coincident with a small pop-in load drop, in an otherwise stable crack growth load-displacement curve. Extensive fractography was performed on both tensile and 3PB specimens to provide insight on the fracture mechanisms at different temperature range using SEM (FEI xL30).

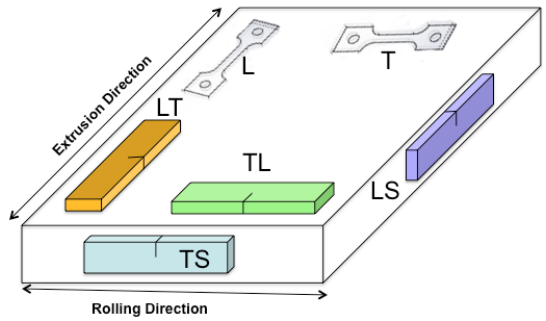

Figure 1. NFA1 test specimen orientations with respect to extrusion and cross-roll directions.

STATUS AND PROGRESS

Microhardness

Vicker's microhardness (H_v) data for several NFA are summarized in Table 1. H_v averages 376 ± 18 (kg/mm^2) for NFA1, which is slightly lower than for PM2 (401 H_v) and higher than for one heat of MA957 (336 Hv), respectively. These differences can probably be partly attributed to the respective alloy grain sizes.

Table 1. Microhardness and grain size of NFA1, PM2 and MA957.

Materials	NFA1	PM2	MA957
Grain Size (nm)	454	424	1470 x 630
Microhardness (Hv)	376 ± 18	401 ± 15	336 ± 8

Tensile Properties

NFA1 tensile properties are summarized in Figure 2 both for L and T orientations from ≈ 22 to 800°C. The alloy is both strong and ductile with little to modest effects of orientation. However, the overall the L orientation has slightly better properties than in the T orientation. The tensile properties are typical of NFA.

SEM fractographs for the L orientation reveals dimple-like features for all the samples confirming ductile fracture (Figs. 3a, 3b and 3c). Room temperature fracture sample showed large flat dimples. Surface cracks formed parallel to the loading direction (Figure 3d). The dimples are much finer at 400°C and the surface cracks have directions both somewhat parallel and angled with respect to the tensile axis (Figs. 3b and 3e). Typical microvoid coalescence is also observed at 800°C but details are masked by extensive oxidation, while crack are observed perpendicular to the loading axis (Figs. 3c and 3f). Macroscopic views of the fracture surface are shown in Figs. 3g, 3h and 3i. At 22°C, a large amount of necking is observed and the surface cracks are seen to connect with through thickness delaminations parallel to the thin dimension of the gauge section. At 400 and 800°C there is slightly less necking and no delaminations are observed. Generally similar observations apply to tensile tests in the T orientation. Figure 4 shows the geometry of the delaminations observed at 22°C in both orientations.

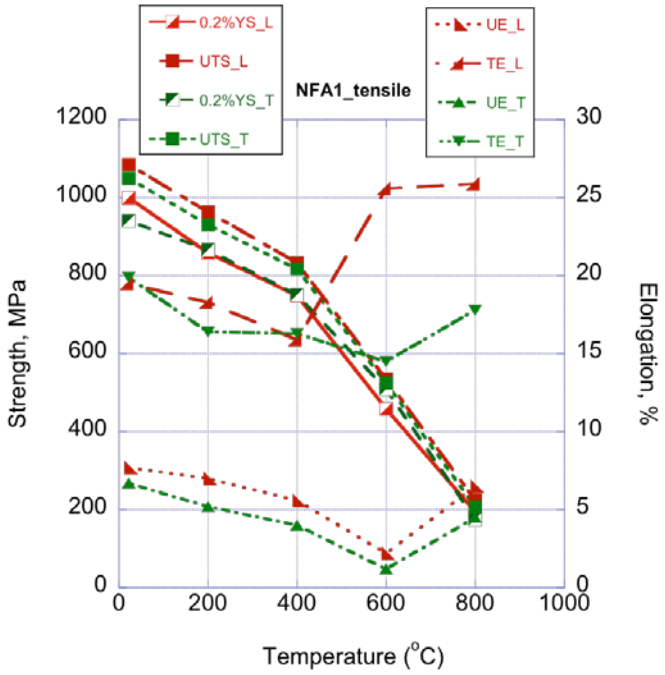

Figure 2. Tensile properties of NFA1 in the L and T orientations as a function of temperature.

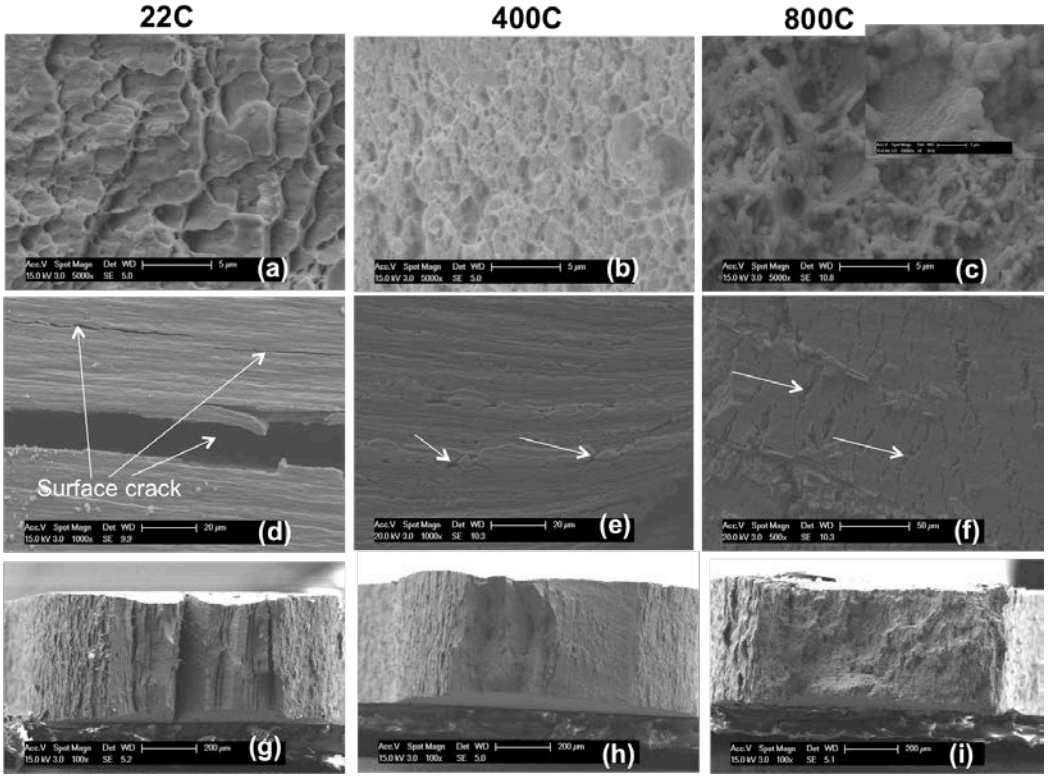

Figure 3. SEM fractographs of NFA1 showing: (a-c) shear-lips @ 22°C, (b) dimples at 400°C and (c) microvoid coalescence at 800°C, respectively; (d-f) wide direction surface cracks; and, (g-i) a macro-view of the fracture surfaces.

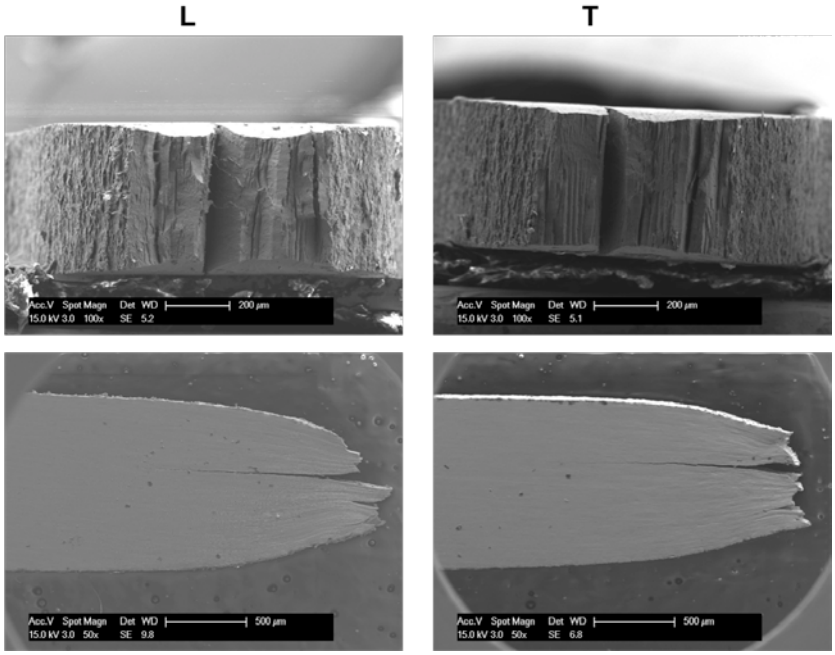

Figure 4. Delamination in the L and T orientations at room temperature.

Fracture Toughness

Typical fracture load displacement curves are illustrated in Figure 5. Figure 5a shows a load displacement curve characteristic of tests at all but the lowest temperature, indicating stable crack growth signaled by a gradually decreasing post maximum load. Figure 5b shows a load displacement curve for linear elastic brittle fracture at -196°C. The fracture toughness (K_{Jc}) results are shown in Figure 6. The upper shelf toughness lies in the vicinity of 100 MPa√m, indicating only modest tearing resistance compared to conventional 9Cr tempered martensitic steels. However, the transition from ductile tearing to cleavage initiation takes place at a remarkably low temperature at (LT) and (TL) below ≈ -175°C. There is little effect of specimen orientation. This can be attributed to the nearly equiaxed grain morphology of NFA1 in the crack propagation plane [2]. However, on average the upper shelf toughness and transition temperature are both slightly higher in the LT orientation.

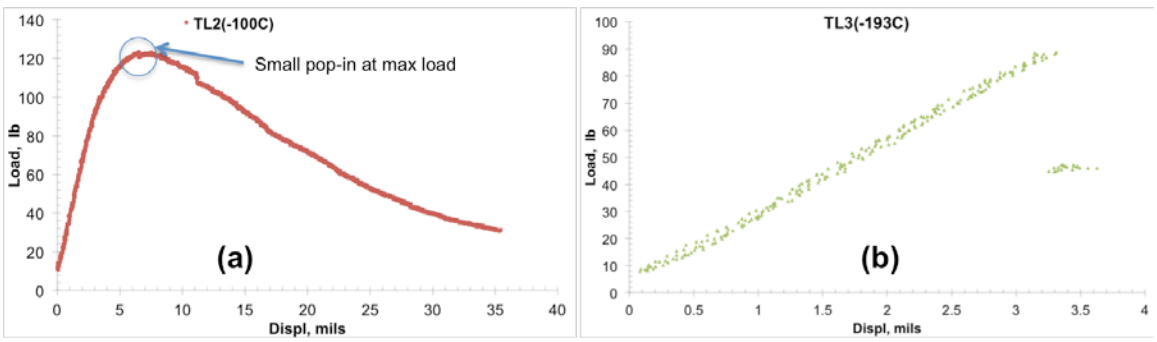

Figure 5. Load-displacement curves of TL 3PB fracture samples at: (a) -100°C and (b) -196°C, respectively.

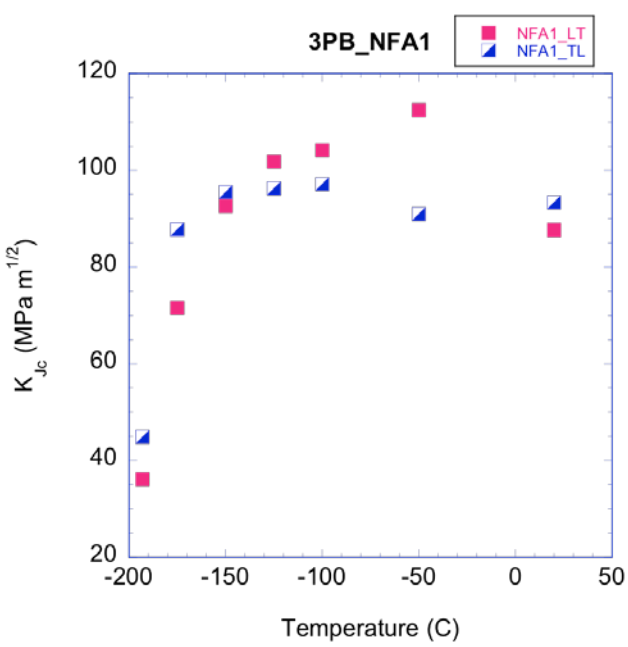

Figure 6. Fracture toughness of FCRD NFA1 as a function of test temperature.

Figure 7 shows the macroscopic view of the fractured surfaces in the two orientations and at various temperatures. The fractured surfaces are dominated by the delaminations (splits) from room temperature down to -150°C (LT) and -175°C (TL) orientation. Shear lips and dimple ductile microvoid coalescence is observed between the delaminations that grow in plane parallel to and out of plane perpendicular to the crack propagation direction. The delamination planes are perpendicular to both the extrusion and cross rolling directions, likely along prior particle boundaries between the broader faces of the compressively deformed powders.

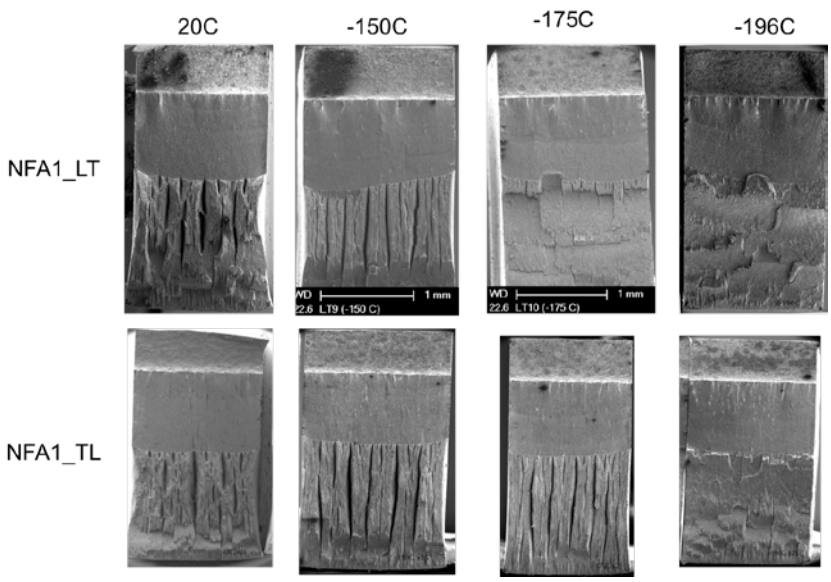

Figure 7. SEM fractographs of NFA1 fracture surfaces both for LT and TL orientations.

These observations provide insight on the reason for the low transition temperature in FCRD NFA-1. The initial lateral triaxial stress component parallel to the crack front is sufficient to cause the delaminations. However once the delaminations occur the lateral stress is relaxed and deformation occurs under plane stress rather than plane strain conditions resulting in a major decrease in the crack tip stress fields and much higher toughness by a ductile rather than a cleavage mechanism. However, at the lowest temperature cleavage initiation occurs before delamination.

Discussion and Summary

We believe that the properties of NFA1 represent a truly extraordinary, and perhaps unique, combination of high strength, ductility and fracture toughness. The high strength is provided by a combination of small grains, high dislocation densities and a very large number of nano-oxide dispersion strengthening features. These properties are remarkably isotropic in the key orientations pertinent to structural performance. Perhaps the most notable property is the fracture toughness with a transition to cleavage fracture at or below ≈ -175°C. Perhaps the main contribution to high toughness is triaxial stress driven delaminations that alter the blunting crack tip stress fields from plain strain to plane stress states. A further beneficial attribute of NFA1 (and other alloys in this class) is its ability to sustain stable crack growth up to very large amounts of deformation. That is cracked structures will be highly ductile, and thus forgiving in service. Further, while the tearing toughness is modest the load capacity of NFA1 will be close to net section limit conditions as governed yield and flow stress constitutive properties. However, it must be emphasized that we have explored mainly low temperature or static properties. Future research will emphasize: a) time-dependent, high temperature properties including creep crack growth; b) development of fully microstructurally informed micormechanical models or NFA deformation and fracture; c) optimization of NFA to further improve their mechanical properties; and, d) detailed evaluation of the advantages and disadvantages of NFA under realistic in service structural applications.

Acknowledgments

This work is part of a multi-laboratory collaboration between LANL, UCSB and ORNL. The DOE Office of Fusion Energy Sciences supported some of the mechanical testing reported here. NFA-1 was produced with the sponsorship of the DOE Office of Nuclear Energy under both a NEUP grant and the FCRD program.

REFERENCES

[1] G.R. Odette, D.T. Hoelzer, "Irradiation-tolerant nanostructured ferritic alloys: Transforming helium from a liability to an asset," JOM. 62, 84 (2010).

[2] N.J. Cunningham, Y. Wu, G.R. Odette, D.T. Hoelzer, S.A. Maloy, " Characterization of a larger best practice heat of 14YWT in annealed powder, HIP consolidated and extruded forms," DOE/ER-0313/54 (2013), DOE Fusion Reactor Materials Program Semiannual Progress Report (2013).

[3] N.J. Cunningham, Y. Wu, G.R. Odette, D. Gragg, K. Field, D.T. Hoelzer, S.A. Maloy, "Characterization of the final precursor alloy to a larger best practice heat of 14YWT," DOE/ER-0313/53 (2012), DOE Fusion Reactor Materials Program Semiannual Progress Report (2012).